Eur. Phys. J. B **34**, 257–263 (2003)
DOI: 10.1140/epjb/e2003-00219-y

THE EUROPEAN PHYSICAL JOURNAL B

On the dechanneling of protons in Si [110]

M. Kokkoris[1,a], G. Perdikakis[1], S. Kossionides[1], S. Petrović[2,b], and E. Simoen[3]

[1] Institute of Nuclear Physics, Tandem Accelerator, NCSR 'Demokritos' 15310, Aghia Paraskevi, Athens, Greece
[2] Laboratory of Physics, Vinča Institute of Nuclear Sciences, PO Box 522, 11001 Belgrade, Yugoslavia
[3] IMEC, Kapeldreef 75, 3001 Leuven, Belgium

Received 12 May 2003
Published online 11 August 2003 –

Abstract. In the present work, the dechanneling of protons in Si [110] is studied combining theoretical Monte-Carlo and phenomenological simulation results in the energy range $E_p = 1.8 - 2.4$ MeV. The applicability of a Gompertz type sigmoidal dechanneling function, with two parameters, k and x_c, which represent characteristic dechanneling rate and range, respectively, is examined, yielding the successful reproduction of backscattering spectra of channeled protons along the Si [110] crystal axis. The results are compared to the ones obtained in the past for different beam – crystal orientation combinations and an attempt is made to explain the occurring similarities and discrepancies.

PACS. 61.85.+p Channeling and related phenomena – 61.80.Jh Ion radiation effects

1 Introduction

The problem of the dechanneling of ions, *i.e.* the transition of the channeled ions into nonchanneled ones as they penetrate into the crystal, has been studied since the early days of channeling in order to accurately reproduce the experimental channeling spectra in the backscattering geometry [1–4]. Such an accurate description has profound consequences in both the scientific and the technological context [5].

Theoretical calculations concerning the dechanneling mechanism are based either on the analytical description of ion channeling in crystals, founded by Lindhard [6], or on the Monte Carlo numerical method, founded by Barrett [7]. Lindhard's approach used the formalism of statistical mechanics, including the continuum approximation and the assumption of a statistical equilibrium in the transverse plane. Barrett's numerical approach used ion-atom scattering theory and a computer simulation method for three-dimensional following of ion trajectories in crystal channels. Although this approach is more complex, a number of calculations have shown that it is more accurate than Lindhard's one. As a clear example, Krause *et al.* [8] obtained coincidence of the experimental and calculated angular distributions of 2–9 MeV protons and 6–30 MeV C^{q+} ions ($q = 4$–6), channeled in thin Si [100] crystals, using Barett's approach, while Lindhard's approach would have given qualitatively different angular distributions.

In the analytical approach, a simple exponential behavior of the dechanneling function, *i.e.*, dechanneling fraction of ion beam inside the crystal as a function of crystal depth, has been derived with the assumption of constant dechanneling rate [9,10]. More accurate description of the dechanneling process requires solution of a diffusion type differential equation (Fokker-Planck equation) with exact coefficients [11–14]. Recently, an interesting attempt was presented, concerning proton dechanneling in a diamond crystal [15]. Nevertheless, to the authors' best knowledge, an accurate reproduction of experimental channeling spectra in the backscattering geometry with the implementation of diffusion models is still lacking.

Simulations of spectra in RBS channeling experiments have also been reported using Monte Carlo calculations [16,17] or phenomenological approaches [18,19] with varying success. The phenomenological attempts were mainly based on the assumption of a constant dechanneling rate, *i.e.* an exponential dechanneling function [19]. Although certain aspects of the channeling spectra have been reproduced both qualitatively and quantitatively well, the complete understanding of the dechanneling process has not yet been achieved.

In the present work, the dechanneling process in the case of protons, in the energy range $E_p = 1.8$–2.4 MeV, channeled in a Si [110] crystal shall be analyzed, combining theoretical Monte-Carlo results with a phenomenological approach, in order to accurately describe the dechanneling mechanism through a simple analytical form of the dechanneling function. The Gompertz type sigmoidal

[a] e-mail: kokkoris@inp.demokritos.gr
[b] e-mail: petrovs@vin.bg.ac.yu

dechanneling function with only two parameters, k and x_c, denoting the characteristic dechanneling rate and range respectively, leads to an accurate reproduction of RBS channeling spectra. It also provides a valuable insight of the dechanneling mechanism. The results are compared to the ones obtained in the past, concerning channeling parameters for different beam – crystal orientation combinations in the same energy range, and an attempt is made in order to explain the occurring similarities and discrepancies.

2 Theoretical approach – Monte-Carlo calculations

In order to study theoretically the dechanneling process, a Monte-Carlo simulation code based on the continuum approximation has been used. This code has already been successfully used for the analysis of the angular distributions and transmission patterns of channeled ions, and it has been described in detail elsewhere [20,21]. The trajectory of a channeled ion is followed *via* the numerical solution of its equations of motion in the transverse plane. The continuum interaction potential of the ion and an atomic string of the crystal is derived from Moliere's approximation of the Thomas-Fermi ion-atom interaction potential [8,20,21]. Thomas-Fermi screening radius $a = [9\pi^2/(128Z_2)]^{1/3}a_0$, where Z_2 is the atomic number of atoms in the crystal, and a_0 is Bohr radius, was used following the experience of Krause *et al.* [8]. Effects of energy loss and electron multiple scattering of the channeled ions were taken into account [21]. The effect of thermal vibrations of the target atoms was included for the continuum potential of the ith atomic string as:

$$U_i^{th} = U_i + \frac{\sigma_{th}^2}{2}(\partial_{xx}U_i + \partial_{yy}U_i), \qquad (1)$$

where U_i is the continuum potential of the ith atomic string with the thermal vibrations of the atoms neglected, and σ_{th} is the one-dimensional thermal vibration amplitude of the atoms [20,21], but the uncertainty of the scattering angle of the ion caused by the effect of thermal vibrations of the atoms of the crystal was not included in the code. The use of expression (1) is justified when the distance between the ion and the atomic string is large compared to the one-dimensional thermal vibration amplitude [22]. The continuum potential of the crystal is the sum of the continuum potentials of the atomic strings. Angular divergence of the ion beam was also taken into account [21].

In the case under consideration *i.e.*, Si [110] crystal, the channel is rhombic with two atomic strings per vertex of the rhomb. The atomic strings lying on the two nearest (relative to the channel axis) rhombic coordination lines were taken into account. The one-dimensional thermal vibration amplitude of the crystal atoms (for room temperature) was taken to be 0.00744 nm [23]. Calculated screening radius was 0.0194 nm. The thickness of one atomic layer of the crystal, d, was 0.384017 nm [24]. Critical angles for channeling $\Psi_c \equiv \left(2Z_1Z_2e^2/E_pd\right)^{1/2}$, where Z_1 is atomic number of projectile (proton), for the energy range of protons into consideration, $E_p = 1.8$–2.4 MeV, were in the range of $\Psi_c = 7.86 - 6.61$ mrad, respectively. A proton was considered to be dechanneled, at a certain crystal depth, if its angle with the channel axis was larger than the critical one. The cut-off energy was set to $E_p/3$, *i.e.*, protons at large crystal depths whose energies were less then the one third of the initial energy were not taken into account. Also, protons whose initial impact parameters were less than the screening radius were treated as backscattered. The initial number of protons was ~ 5000 and it was chosen considering optimum computing time and statistical accuracy.

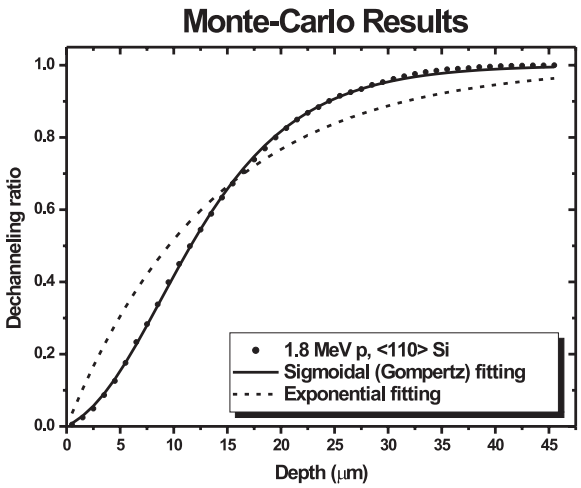

Fig. 1. Monte-Carlo results showing the dechanneling ratio for 1.8 MeV protons channeled along the Si [110] crystal axis, as well as, sigmoidal and exponential fitting curves. The Gompertz type sigmoidal fitting function reproduces the results much more accurately than the simple exponential one.

Figure 1 shows the calculated dechanneling function in the case of 1.8 MeV protons. The angular divergence of the proton beam was taken to be 0.3 mrad. It is clear from Figure 1 that the dechanneling function is a sigmoidal one. In order to find an analytical expression that approximates this dechanneling function, Gompertz type sigmoidal function was adopted:

$$N_d = N_o \cdot \frac{e^{-\exp(-k\,(x-x_c))} - e^{-\exp(kx_c)}}{1 - e^{-\exp(kx_c)}} \qquad (2)$$

where N_d is the number of dechanneled ions, N_o is the initial number of ions, x is the crystal depth, k and x_c are fitting parameters representing the characteristic dechanneling rate and range, respectively; it is assumed that the initial number of dechanneled ions is zero and that it approaches N_o for very large crystal depths. The Gompertz type sigmoidal function, obtained in a fitting procedure in which the fitting parameters are varied in order to find the best approximation of the dechanneling function, is shown in Figure 1. As a comparison, the simple

exponential approximation of the dechanneling function, given by the expression:

$$N_d = N_o \cdot \left(1 - e^{-kx}\right) \tag{3}$$

where k is a constant (dechanneling rate independent of crystal depth), is also shown in Figure 1. It is clear that the Gompertz type sigmoidal function is both quantitatively and qualitatively a much better approximation than the exponential one.

Analysis of expression (2) shows that the parameter x_c corresponds to the inflection point of the sigmoidal function and, thus, it can be attributed to the characteristic dechanneling range. Also, the distribution of the number of dechanneled protons per unit length as a function of crystal depth, shown in Figure 2, is asymmetric, has a maximum at inflection point x_c, a fast rise for $x < x_c$ and a slow decay (tail) for $x > x_c$. The dechanneling rate, *i.e.* the probability for dechanneling per unit crystal depth, in the case of Gompertz type dechanneling function (2), is given by:

$$-\frac{1}{N_c}\frac{dN_c}{dx} = \frac{ke^{-k(x-x_c)}}{e^{\exp(-k(x-x_c))} - 1} \tag{4}$$

where $N_c = N_o - N_d$ is the number of channeled ions. Analysis of expression (4), for the cases under consideration, shows that the dechanneling rate is a positive, increasing function, with a horizontal asymptote equal to k. This behavior of the dechanneling rate, as well as, of the distribution of the number of dechanneled protons per unit length, can be explained with impact-parameter (trajectory) dependence of the dechanneling process, *i.e.*, with the fact that the ions with initially small impact parameters (relative to an atomic string) dechannel much faster than the ones with initially large impact parameters. For large crystal depths (a few times larger than x_c), the channeled fraction of the beam consists mostly of ions being initially around the channel axis and the dechanneling process is characterized by an almost constant (slowly changing) dechanneling rate. Thus, the parameter k represents the characteristic dechanneling rate, corresponding to large crystal depths and to ions initially being around the channel axis. Figure 2 also shows a comparison between two curves, one corresponding to the Gompertz type dechanneling function (2) and one following the Boltzmann type sigmoidal dechanneling function:

$$N_d = N_0 \frac{e^{k(x-x_c)} - e^{-kx_c}}{1 + e^{k(x-x_c)}} \tag{5}$$

with two fitting parameters, x_c and k, having the same interpretation as in the Gompertz case. Both curves were obtained in a fitting procedure in which the parameters are varied in order to find the best approximation of the dechanneling function. It is clear that the Gompertz type dechanneling function describes the dechanneling process better than the Boltzmann one.

It should be noted, that inclusion in the Monte Carlo code of the uncertainty of the scattering angle of the ion caused by the effect of thermal vibrations of the atoms of the crystal would not qualitatively change the energy dependence of the characteristic dechanneling parameters, since it has the same energy dependence ($\approx 1/E$) as the electron multiple scattering effect. Moreover, in all cases analyzed in the present work, most of the ions experience collisions with the atomic strings at distances larger than the one-dimensional thermal vibration amplitude of the crystal atoms (at room temperature), in accordance with the use of expression (1).

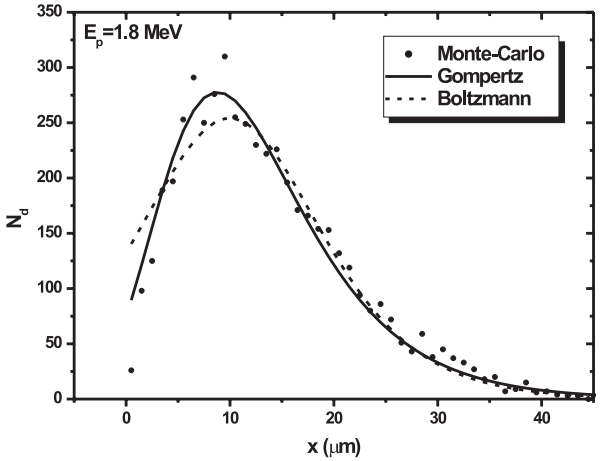

Fig. 2. Monte-Carlo results showing the number of dechanneled ions per unit length as a function of crystal depth, as well as, the corresponding Gompertz and Boltzmann curves. The Gompertz curve is clearly a better approximation to the theoretical results.

3 Phenomenological approach

A new phenomenological approach was proposed recently, based on the use of a nuclear resonance as a marker for the crystal depth [19], and on the assumption of an exponential dechanneling function of the ions inside crystal channels [10]. The observation of nuclear reaction yield in channeling is attributed to the dechanneling of protons after they travel for a distance along the channel axis. This approach led to the successful simulation of channeling backscattering spectra in the systems p+^{28}Si [100] [19], p+^{28}Si [111] [25], p+SiO_2 (c-axis) [26], and p+SiC [0001] [27].

In that approach, the dechanneling process was defined by only two parameters, α, the ratio of stopping powers in the channeling and random directions (taken as a constant over the energy range in which the particle travels inside the channel) and $\lambda \equiv 1/k$, the mean channeling distance, where k is the dechanneling rate (constant). This technique allowed *in situ* measurements and could be applied to several bulk single crystals (simple or compound) without any particular sample preparation, combining NRA and channeling. The existence of a resonance in the spectrum however, was not an absolute requirement, although it increased the accuracy of the results. It should be noted here that the values reported for α corresponded to the average trajectories of channeled ions.

The method used for the simulation of the energy spectra has been described in detail elsewhere [19]. The basic assumption was that beam particles dechannel exponentially (3). However, one can assume a Gompertz type sigmoidal behavior (2) for the dechanneling of the incoming beam, as suggested from the Monte-Carlo simulation results, and that can also be incorporated in the algorithm.

The part of the beam that has been dechanneled, is considered to lose energy at a rate corresponding to the one calculated with the coefficients of Ziegler [28] in the random direction, while the part of the beam still channeled is considered to lose energy at a fraction of that rate. Thus, specific channeling energy loss is given by:

$$S_{channel}(E) = \alpha \cdot S_R(E) \tag{6}$$

where α is assumed to be energy independent, and $S_R(E)$ is the specific energy loss in the random direction. The validity of this hypothesis has been discussed analytically in the past [27]. It should be noted here, that although α is expected to decline with energy [29], previous experiments did not show a consistent variation with energy in the range of 1–2.5 MeV/amu [30]. An analytical expression for α – if established – could be incorporated in the simulation algorithm, but the quality of the simulated spectra in several crystals studied using this method, showed that this first-order approximation of a constant α value is valid for the energy interval into consideration. For the calculations, the target was divided into slices of thickness $dx = 20$ μg/cm^2 ($\sim$ 862 nm), and the beam was split into two components, a channeled and a dechanneled one. The evolution of each component was then followed throughout the target.

For the simulation of the experimental spectra, the accurate knowledge of the energy dependence of the elastic cross section of the reaction ^{28}Si(p,p)^{28}Si is mandatory. Thus, the excitation function was obtained from the literature [31] for the laboratory angle into consideration. The effect of the beam straggling was accounted for, using Bohr's equation, but not the multiple scattering effect, which is important at low energies. The initially dechanneled part of the beam (2–4%, as determined by the χ_{min} from the RBS/C spectra) was taken into account. The excitation function used, reproduced the spectra in the random direction within 5–7% accuracy, and was thus subsequently used for the simulation of the corresponding channeling spectra. The problem of the cross section used in NBS is a crucial limiting factor for the accuracy of the results. It should be also noted that the depth resolution of this technique strongly depends on the characteristics of any existing resonances, typically varying between 1000–2000 nm for the energy range into consideration.

Therefore, with given α and λ, in the case of exponential dechanneling, and α, k and x_c, in the case of Gompertz type sigmoidal dechanneling, simulated channeled spectra can be generated and compared to the experimental ones. The best possible fit is determined after χ^2 minimization, using the code MINUIT developed at CERN.

4 Experimental procedure

The experiments were performed at N.C.S.R 'Demokritos', Athens, Greece, using the 5.5 MV T11 TANDEM Accelerator. Protons were accelerated to energies $E_p = 1.8 - 2.4$ MeV and were lead to a scattering chamber (RBS-400 by Charles Evans Co), which included a 4-motor goniometer system capable of determining the target orientation with an accuracy of 0.01°. The detection system consisted of a single Si surface barrier detector, placed at an angle $\Theta_{lab} = 170°$ with respect to the beam, having an overall resolution of 12 keV for α-particles (8 keV for protons). The beam divergence was less than 0.02° ($\sim$ 0.3 mrad) due to the long collimation system (consisting of two 1.5 mm collimator apertures having a distance of 3.5 m between them and 60 cm between the antiscatterer and the target). The vacuum pressure was kept constant during the measurements (5×10^{-7} mbar). The amorphous carbon deposition on the target's surface was negligible. This was verified in the experimental channeling spectra by the absence of a particularly strong resonance signal in the p+^{12}C system at $E_p = 1.75$ MeV [32], monitored during the process. The beam spot size was approximately 2×2 mm^2 and the beam current did not exceed 5 nA on target.

The target used was a Czochralski Si crystal wafer provided by IMEC, boron doped to a resistivity of $10-15$ $\Omega\cdot$ cm, cut normally to the plane (110). Before all the measurements the wafer was boiled in acetone for 5 min for the removal of all the biological contaminants and was dipped for 10 s into a 5% HF solution for the removal of the native oxide. Subsequently, a polar and an angular scan were performed in order to align the beam to the [110] axis of the crystal. The channeling angle was found to be approximately 0.3°. For the polar scan, the target was tilted by 3° and rotated around the beam axis. The fine-tuning of the channeling position was finally achieved *via* an angular scan. Due to the high inflicted dose and in order to avoid any radiation damage effects coming from the trace region of the implanted protons, the channeling spectra were acquired at several positions on the wafer, differing by at least 2 mm. The excellent crystalline behavior of the sample is demonstrated in Figure 3a where the RBS/C spectra are presented at $E_p = 1.5$ MeV. The χ_{min} was less than $\sim$2% in the whole energy range.

Spectra of protons backscattered at an angle Θ_{lab}=170° were taken within the energy interval, E_{lab} = 1.8–2.4 MeV, in steps of 50 or 100 keV, for the same accumulated charge of 4 μCb, in both random and aligned angles of incidence. The reaction ^{28}Si(p,p)^{28}Si exhibits two sharp resonances in that energy interval, at energies $E_{lab} = 1.67$ MeV and 2.09 MeV, having natural widths of $\Gamma = 52.0 \pm 0.8$ and 15.6 ± 0.6 keV, respectively. The shape of the spectra as well as the differences between the channeling and the random mode are shown in Figure 3b for $E_p = 2.15$ MeV. The interference patterns between the compound and the direct elastic (Rutherford) scattering are evident. The 1.67 MeV resonance is diffused, due to

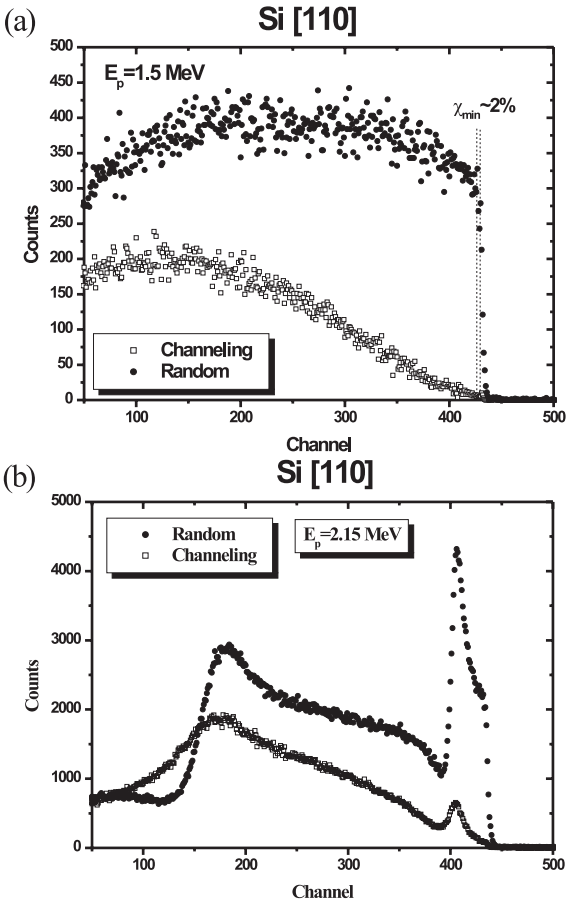

Fig. 3. (a) RBS/C spectra at $E_p = 1.5$ MeV showing the excellent crystalline quality of the target, yielding a $\chi_{min} \sim 2\%$ (b) RBS/C spectra at $E_p = 2.15$ MeV showing the resonance interference patterns. The 2.09 MeV resonance appears clearly close to the surface, while the 1.67 one is diffused at greater depths.

the effect of energy straggling at greater depths, while the 2.09 MeV one appears sharp, closer to the surface.

5 Experimental results and discussion

The choice of Si [110] for the assessment of the precise dechanneling function originated from geometrical considerations, since this crystallographic orientation represents the largest channel in Si. Therefore, any discrepancies from the exponential dechanneling function would be easily monitored. And indeed, as it was mentioned in previous publications concerning the [100] and [111] orientations [19,25], there were small discrepancies near the crystal surface, or at small depths, as well as at large depths, indicating the existence of a more complicated dechanneling function. The excellent crystalline quality of the Si [110] crystal, and its crystallographic geometry, revealed that the sigmoidal approach (Gompertz type sigmoidal dechanneling function) is much more accurate than the exponential one in reproducing the experimental spectra, as shown clearly in Figure 4a, for $E_p = 1.8$ MeV, where

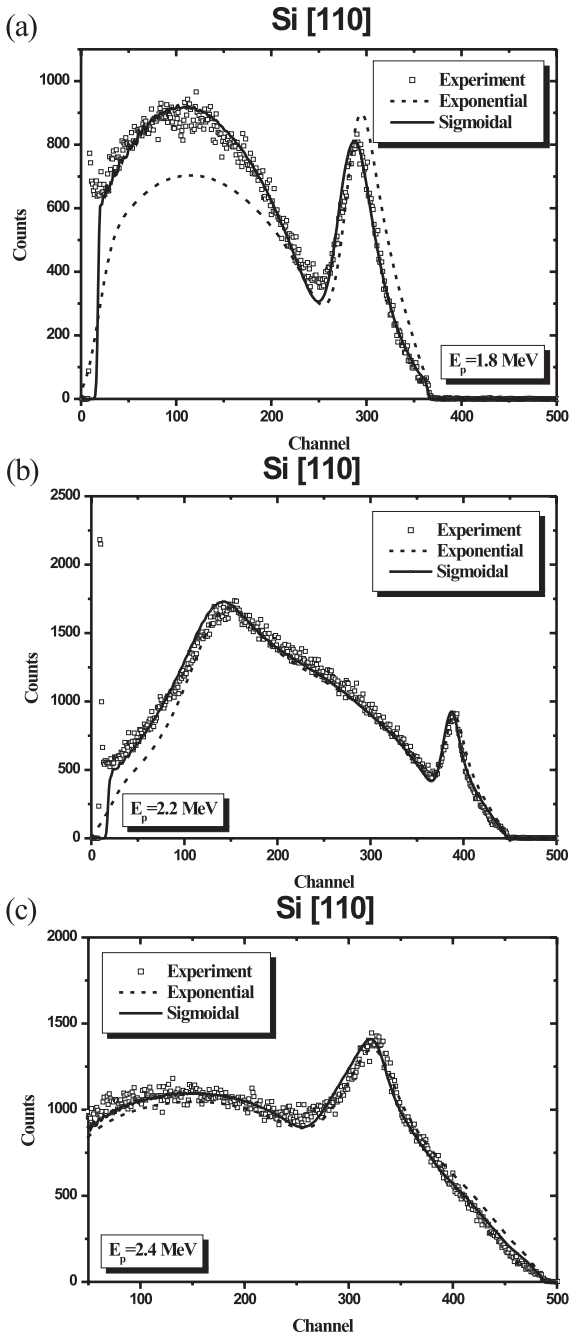

Fig. 4. Experimental channeling spectra in the backscattering geometry, along with the simulation results using the exponential and the Gompertz type sigmoidal dechanneling functions in the cases of: (a) $E_p = 1.8$ MeV, (b) $E_p = 2.2$ MeV and (c) $E_p = 2.4$ MeV.

the 1.67 MeV resonance appears close to the surface. The accuracy of the Gompertz type sigmoidal dechanneling function was observed in all the energy range considered here, although the differences between the two dechanneling functions become less evident at higher energies, as shown in Figures 4b and c, for $E_p = 2.2$ and 2.4 MeV, respectively. This is related to the limitations of the phenomenological approach, as will be analyzed in the following paragraphs.

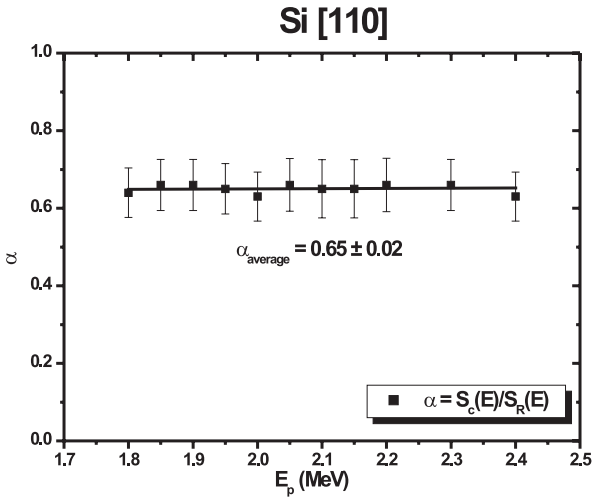

Fig. 5. The stopping power ratio, α, as a function of energy ($E_p = 1.8$–2.4 MeV). The average value determined was 0.65 ± 0.02.

Another interesting result was the invariance of the parameter α with the energy, when the Gompertz type sigmoidal dechanneling function was used, as shown in Figure 5, yielding an average value of 0.65 ± 0.02. It is also interesting that α very weakly depends on the energy when the exponential dechanneling function was used, and did not vary for more than 5% comparing to the values obtained using the sigmoidal dechanneling function. Those results are in very good agreement with values of parameter α reported for the Si [100] and [111] crystals, namely 0.69 ± 0.01 and 0.74 ± 0.01 respectively, using exponential dechanneling function, and provides an indirect, though conclusive proof that α is inherent to the crystal channel axis, having only a weak dependence on the choice of the dechanneling mechanism. This is also in accordance with the assumption that parameter α is energy independent. Nevertheless, since the investigated energy region was rather limited, further work is required, over a broad energy range and with a variety of beam – crystal orientation combinations, before a complete understanding of the behavior of the stopping power ratio is accomplished.

The use of the sigmoidal dechanneling function requires the introduction of two parameters, namely x_c and k. Thus, the simplicity of utilizing only one parameter, λ, denoting the 'mean channeling distance', in the case of the exponential dechanneling function, is lost, but the physical meaning of the two parameters reveals the complexity of the dechanneling process in a more accurate way, as analyzed in the theoretical section. It is also evident, that if one uses a simple exponential formula (3) for the description of the dechanneling process, then, for the χ^2 minimization algorithm to converge, and in order to attain a good simulation at greater depths, the dechanneling of the proton beam near the surface, or at small depths inside the crystal, has to be clearly overestimated, while at greater crystal depths there always exists a slight underestimation (Fig. 1). The weak dependence of the stopping power ratio, α, on the choice of the dechanneling function

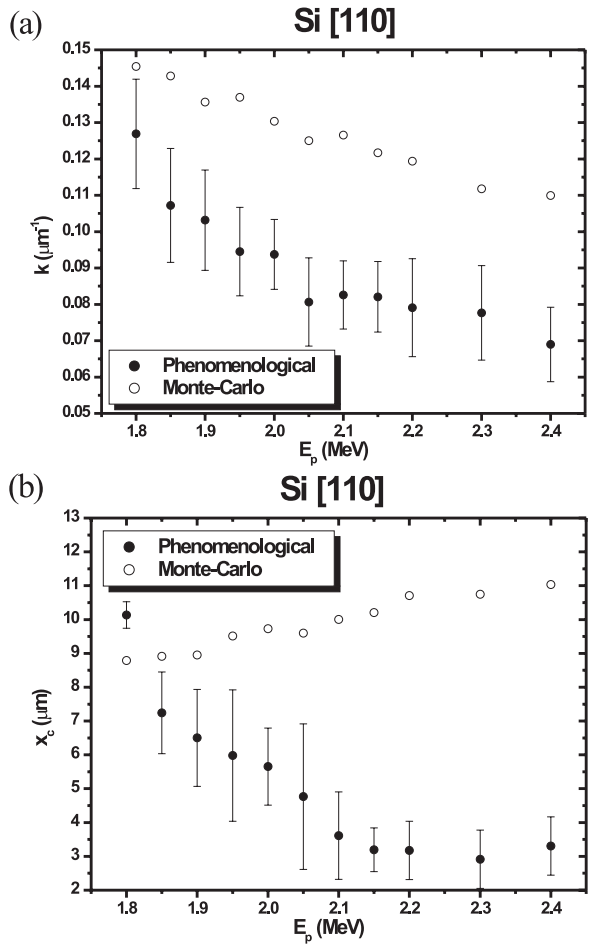

Fig. 6. (a) Dechanneling rate, k, and (b) dechanneling range, x_c, as a function of energy, according to the theoretical and the phenomenological approaches. The experimental errors are indicated in the graphs.

renders the results mentioned in previous works [19,25–28] reliable, but the use of the sigmoidal dechanneling function provides a superior reproduction of the experimental spectra in the simulation procedure, as shown in Figure 4, and should be considered as the key factor for the explanation of discrepancies observed in the past in the cases of α+MgO [100] and α+Al_2O_3 [$0\bar{1}0\bar{2}$] [33].

Nevertheless, if one compares the results of the Monte-Carlo simulation with those of the phenomenological one, concerning the evolution of the dechanneling parameters k and x_c with respect to the proton beam energy, the deviations are large and become even more profound with the increase of energy, as shown in Figures 6a and b. In the case of the characteristic dechanneling rate, k, shown in Figure 6a, the energy trend is the same for both approaches, *i.e.* k is decreasing with energy, but with increasing discrepancies denoting that the phenomenological approach clearly underestimates the 'real' dechanneling rate. For the characteristic dechanneling range, x_c, shown in Figure 6b, the simulation results differ considerably, qualitatively and quantitatively, from the theoretical predictions, suggesting a decrease rather than an increase of x_c with energy. Behind this apparent disagreement lies

the basic limitation of the phenomenological approach, namely the inherent 'mean' or 'single energy' approximation. As was analyzed in the phenomenological section, the channeled beam is considered to be monoenergetic, losing energy at discrete steps. This contradicts the impact parameter (trajectory) dependence of the channeling energy loss, which is related to the impact parameter dependence of electron density in the crystal channel and thus to the number of inelastic ion collisions with the electrons. If one assumes an energy distribution of a Gaussian form for the channeled part of the beam inside the crystal, having a width Γ increasing with depth, then the simulation results converge towards the Monte-Carlo ones. This, however, requires the introduction of additional parameters in the fitting procedure, thus impeding its applicability and usefulness. It is also evident, that the smearing out of the differences between the spectra at high energies, obtained using the exponential and the sigmoidal dechanneling functions, as illustrated in Figure 4, can be entirely attributed to this fundamental issue.

6 Conclusions

In the present work, the Gompertz type sigmoidal dechanneling function, with two parameters, k and x_c, representing characteristic dechanneling rate and range, respectively, was introduced and analyzed both by theoretical, Monte-Carlo calculations, and by a phenomenological model. The simulation results clearly demonstrate that the sigmoidal dechanneling function can accurately describe the dechanneling of protons impinging along the Si [110] crystal axis, and thus it is superior to the simple exponential one in reproducing the experimental channeling spectra in the backscattering geometry. At the same time, it offers a valuable insight concerning the understanding of the dechanneling mechanism.

The differences between the theoretical predictions and the simulation results concerning the energy dependence of parameters k and x_c, are attributed to the basic limitation of the phenomenological approach, namely the 'mean' or 'single energy' approximation of the channeled part of the beam inside the crystal. Moreover, α, the stopping power ratio, remains stable within 5% for the energy range into consideration ($E_p = 1.8$–2.4 MeV), and is only weakly dependent on the choice of the dechanneling function.

Although the sigmoidal dechanneling function has been proven effective, it is the authors' firm belief that further experimental and theoretical work with a variety of beams and crystals is required, before a complete understanding of the dechanneling mechanism is accomplished.

References

1. G. Foti, F. Grasso, R. Quattrochi, E. Rimini, Phys. Rev. B **3**, 2169 (1971)
2. J.A. Davies, L.M. Howe, D.A. Marsden, J.L. Whitton, Rad. Eff. **12**, 247 (1972)
3. A. Fontell, E. Arminen, E. Leminen, Rad. Eff. **12**, 255 (1972)
4. D.S. Gemmell, Rev. Mod. Phys. **46**, 129 (1974)
5. L.C. Feldman, J.W. Mayer, S.T. Picraux, *Materials Analysis by Ion Channeling* (Academic Press, New York, 1982)
6. J. Lindhard, K. Dan. Vidensk. Selsk., Mat-Fys. Medd. **34**, No. 14 (1965)
7. J.H. Barrett, Phys. Rev. B **3**, 1527 (1971)
8. H.F. Krause, J.H. Barrett, S. Datz, P.F. Dittner, N.L. Jones, J. Gomez del Campo, C.R. Vane, Phys. Rev. A **49**, 283 (1994)
9. R. Hellborg, Physica Scripta **4**, 75 (1971)
10. K. Björkqvist, B. Cartling, B. Domeij, Rad. Eff. **12**, 267 (1972)
11. E. Bonderup, H. Esbensen, J.U. Andersen, H.E. Schiøtt, Rad. Eff. **12**, 261 (1972)
12. M. Kitagawa, Y.H. Ohtsuki, Phys. Rev. B **8**, 3117 (1973)
13. T. Oshiyama, M. Mannami, Phys. Lett. A **81**, 43 (1981)
14. V.V. Beloshitsky, F.F. Komarov, M.A. Kumakhov, Phys. Rep. **139**, 293 (1986)
15. R.W. Fearick, T.E. Derry, J.P.F. Sellschop, Phys. Rev. B **40**, 4289 (1989)
16. M. Vos, D.O. Boerma, P.J.M. Smulders, Nucl. Instr. Meth. B **30**, 38 (1988)
17. G. Lulli, E. Albertazzi, M. Bianconi, G.G. Bentini, R. Nipoti, R. Lotti, Nucl. Instr. Meth. B **170**, 1 (2000)
18. E. Kótai, Nucl. Instr. Meth. B **118**, 43 (1996)
19. X. Aslanoglou, P. Assimakopoulos, M. Kokkoris, S. Kossionides, Nucl. Instr. Meth. B **140**, 294 (1998)
20. S. Petrović, L. Miletić, N. Nešković, Phys. Rev. B **61**, 184 (2000)
21. S. Petrović, S. Korica, M. Kokkoris, N. Nešković, Nucl. Instr. Meth. Phys. Res. B **193**, 157 (2002)
22. B.R. Appleton, C. Erginsoy, W.M. Gibson, Phys. Rev. **161**, 330 (1967)
23. B.W. Batterman, D.R. Chipman, Phys. Rev. **127**, 690 (1962); Ya.S. Umanskii, V.I. Prilepskii, Fiz. Tverd. Tela **7**, 2958 (1966); Sov. Phys. Solid State **7**, 2399 (1966)
24. M.E. Straumanis, E.Z. Aka, J. Appl. Phys. **23**, 330 (1952)
25. X.A. Aslanoglou, A. Karydas, M. Kokkoris, E. Kossionides, Th. Paradellis, G. Souliotis, R. Vlastou, Nucl. Instr. Meth. B **161-163**, 524 (2000)
26. M. Kokkoris, R. Vlastou, E. Kossionides, X.A. Aslanoglou, R. Grötzschel, Th. Paradellis, Nucl. Instr. Meth. B **173**, 411 (2001)
27. M. Kokkoris, S. Kossionides, R. Vlastou, X.A. Aslanoglou, R. Grötzschel, B. Nsouli, A. Kuznetsov, S. Petrović, Th. Paradellis, Nucl. Instr. Meth. B **184**, 319 (2001)
28. J.F. Ziegler, J.P Biersack, U. Littmark, *The Stopping and Range of Ions in Solids*, Vol. 1 of *Stopping and Ranges of Ions in Matter* (Pergamon Press, New York, 1984)
29. J.H.R. dos Santos, P.L. Grande, H. Boudinov, M. Behar, R. Stoll, Chr. Klatt, S. Kalbitzer, Nucl. Instr. Meth. B **106**, 51 (1995)
30. A. Simionescu, G. Hobler, S. Bogen, L. Frey, H. Ryssel, Nucl. Instr. Meth. B **106**, 47 (1995)
31. R. Amirikas, D.N. Jamieson, S.P. Dooley, Nucl. Instr. Meth. B **77**, 110 (1993)
32. Z. Liu, B. Li, D. Duan, H. He, Nucl. Instr. Meth. B **74**, 439 (1993)
33. M. Kokkoris, S. Kossionides, X. Aslanoglou, G. Kaliambakos, T. Paradellis, S. Harissopulos, E.N. Gazis, R. Vlastou, C.T. Papadopoulos, R. Grötzschel, Nucl. Instr. Meth. B **136-138**, 137 (1998)